Oleic acid uptake and binding by rat adipocytes define dual pathways for cellular fatty acid uptake

D. D. Stump,* X. Fan,* and P. D. Berk[1],*,†

Division of Liver Disease, Department of Medicine,* and Department of Biochemistry and Molecular Biology,† Mount Sinai School of Medicine, New York, NY 10029

Abstract Oleic acid (OA) uptake by rat adipocytes and the proportions of intracellular unesterified [^{3}H]OA and its ^{3}H-labeled esters were determined over 300 s. Uptake was linear for 20–30 s, with rapid esterification indicating entry into normal metabolic pathways. Initial rates of OA uptake and its binding to plasma membranes were studied over a spectrum of oleic acid:bovine serum albumin (BSA) ratios, and expressed as functions of unbound OA concentrations calculated with both the 1971 OA:BSA association constants of Spector, Fletcher, and Ashbrook and more recent constants (e.g., the 1993 constants of Richieri, Anel, and Kleinfeld), which generate concentrations 10- to 100-fold lower. In either case, uptake was the sum of saturable and linear processes, with ≥90% occurring via the saturable pathway when the OA:BSA molar ratio was within the physiologic range (0.5–3.0). Within this range, rate constants for saturable transmembrane influx (k_s), calculated from both sets of constants, were similar (2.9 s^{-1}) and were 10- to 30-fold faster than those for nonsaturable uptake (k_{ns} = 0.26–0.10 s^{-1}, $t_{1/2}$ = 2.7–6.6 s, based on the constants of Spector et al. and Richieri et al., respectively). The rate of oleic acid flip-flop into rat adipocytes (k_{ff} = 0.16 ± 0.02 s^{-1}, $t_{1/2}$ = 4.3 ± 0.5 s), computed from published data, was similar to k_{ns}. Thus, OA uptake occurs by both a saturable mechanism and passive flip-flop. This conclusion is independent of the OA:BSA association constants used to analyze the experimental measurements.—Stump, D. D., X. Fan, and P. D. Berk. **Oleic acid uptake and binding by rat adipocytes define dual pathways for cellular fatty acid uptake. *J. Lipid Res.* 2001.** 42: **509–520.**

Supplementary key words diffusion • facilitated transport • flip-flop • kinetics

Studies have identified important roles for unesterified long chain fatty acids (uLCFA) that go beyond their well-recognized functions as energy-dense metabolic substrates, components of more complex membrane lipids, or precursors of important biological mediators such as the prostaglandins. In particular, an increased interest in adipocyte biology has identified uLCFA as important intracellular regulators of gene expression (1–3), with significant implications for adipogenesis and for the clinical syndromes of obesity and non-insulin-dependent diabetes mellitus (4–6). Given these roles, control of their intracellular concentrations through careful regulation of their cellular uptake and efflux would be of great value. However, cellular uptake of uLCFA was long considered an entirely passive, and therefore unregulated, process of relatively little intrinsic interest. Although Abumrad et al. (7) and Abumrad, Park, and Park (8) reported as early as 1981 that uLCFA uptake exhibited the kinetic features of facilitated transport, and several plasma membrane proteins have been identified as putative uLCFA transporters (9–15), the nature of cellular ULCFA uptake remains in dispute. The controversy, which is sometimes framed as a dispute over whether cellular uLCFA uptake is entirely passive or entirely facilitated (16), reflects a fundamental lack of agreement about three distinct issues (17): *i*) the nature and *ii*) the rate of the rate-limiting step, and *iii*) whether membrane proteins play a role in the transmembrane movement of uLCFA (reviewed in 16–23).

Most data that address the first two of these issues come from studies of the rates of entry of uLCFA into synthetic membrane vesicles from media in which albumin was either lacking or was present at low concentrations, so that the resulting uLCFA:albumin molar ratios (ν) and unbound uLCFA concentrations were nonphysiologically high (24–26). Such studies have typically used indirect measures (27, 28), including the rate of acidification of the vesicle interior (24–26), to determine the rate of transmembrane uLCFA movement, and were interpreted as showing that the flux of uLCFA across membranes reflected the passive flip-flop of protonated uLCFA across the lipid bilayer. By using these methods, the rates of uLCFA entry into small unilamellar vesicles were reported as being so rapid that no role for an additional, facilitated uptake process could be envisioned. However, when uLCFA

Abbreviations: BSA, bovine serum albumin; OA, oleic acid; [OA_u], unbound OA concentration; pH_i, pH inside a cell or vesicle; uLCFA, unesterified long chain fatty acids; ν, OA:BSA molar ratio.

[1] To whom correspondence should be addressed at the Division of Liver Disease (Box 1633), Mount Sinai School of Medicine, 1 Gustave L. Levy Place, New York, NY 10029.
e-mail: paul.berk@mssm.edu

Downloaded from www.jlr.org by guest, on June 14, 2012

uptake by rat adipocytes (29), pancreatic β cells (30), and cytotoxic T lymphocytes (31) was studied by the same methods and under similar low albumin conditions, observed rates of cellular uLCFA uptake were orders of magnitude slower than those reported in vesicles.

By contrast, studies of oleic acid (OA) uptake by many cell types (32–44), performed with tracer methodology at physiologic albumin concentrations and uLCFA:bovine serum albumin (BSA) molar ratios ($\nu \leqslant 3.3$), found that the principal OA uptake process was a saturable function of the unbound OA concentration ($[OA_u]$). Subsequent studies of hepatocytes, conducted over a much wider range of ν values, specifically identified both saturable and nonsaturable OA uptake components (45). In these cells, for $\nu = 0.5–3.0$, ⩾90% of uptake is via the saturable pathway. As ν increases, the proportion of uptake that is saturable decreases steadily, eventually becoming small at $\nu \geqslant 6:1$. These studies imply that saturable uptake would be a vanishingly small fraction of total uLCFA uptake at the high values of ν used in most studies of uLCFA flip-flop. This suggests *i*) that differences in the nature of the uptake process reported in various studies might simply reflect whichever process predominates under the particular experimental conditions used, and *ii*) that the nonsaturable uptake process observed at high values for ν in our hepatocyte studies (45) reflects the same process described as flip-flop in liposomes and certain cell types. A study by Civelek et al. (29) of OA flip-flop into isolated rat adipocytes provided an opportunity to test this hypothesis.

Accordingly, we have reexamined the kinetics of OA uptake by rat adipocytes over an expanded range of OA concentrations and ν values. These were augmented with studies *i*) of [^{3}H]OA binding to plasma membranes isolated from the same populations of adipocytes, to permit calculation of the separate rate constants for the saturable and nonsaturable transmembrane movement of OA, using the model previously described in hepatocytes (45); and *ii*) of intracellular esterification to document that the OA taken up in these studies had actually entered into intracellular metabolic pathways. In addition, as suggested by Hamilton and Kamp (16), values for $[OA_u]$ required for the analysis of these experiments were computed from both the 1971 OA:BSA binding constants of Spector, Fletcher, and Ashbrook (46) and from the 1993 constants of Richieri, Anel, and Kleinfeld (47). Although the latter yield $[OA_u]$ values roughly 1–2 orders of magnitude lower than the former, comparison of the results confirms that the basic physiologic interpretation of our studies is not dependent on use of a particular set of OA:BSA binding constants.

MATERIALS AND METHODS

Adipocyte plasma membranes

Adipocytes were isolated from epididymal fat pads of male Sprague-Dawley rats by collagenase perfusion (34). The freshly prepared adipocytes were washed twice in Krebs-Ringer-Henseleit buffer, resuspended in homogenizing buffer [0.25 M sucrose, 20 mM Tris-HCl (pH 7.5), 1.0 mM ethylenediaminetetraacetic acid (EDTA)], and homogenized in a Dounce homogenizer (8). After centrifugation the pellet was resuspended in the homogenizing buffer and homogenized once again. The homogenate was layered on top of a solution containing 40% sucrose, 10 mM Tris-HCl (pH 7.5), and 0.5 mM EDTA and centrifuged at 125,000 *g* for 60 min (48). The plasma membranes recovered from the top of the sucrose layer were tested for purity by quantification of the marker enzymes 5′-nucleotidase, cytochrome *c* reductase, and phosphodiesterase and stored at −80°C until used for binding measurements.

OA binding by adipocyte plasma membranes

OA partitioning between BSA and the plasma membrane was measured using minor modifications of a technique previously reported in detail from our laboratory (9, 45, 49, 50). Specifically, aliquots of the plasma membrane preparation containing 240 μg of protein were incubated with 0.6 ml of various concentrations of [^{3}H]OA (Sigma, St. Louis, MO) bound to 33 μM [^{14}C]BSA (Sigma) in phosphate-buffered saline (PBS). The final molar ratio of plasma membrane phospholipid to BSA was approximately 8:1, well within the range in which we have previously demonstrated the partition ratio of OA to be independent of the plasma membrane phospholipid:BSA ratio (45). The final equilibrium OA:BSA ratios in solution ranged from 0.125 to 3.84. The plasma membranes were incubated with the OA:BSA solutions for 30 min at 37°C (measurements of binding at 0, 5, 15, 30, 60, and 120 min revealed that there was no change in the OA bound to the plasma membrane from 15 to 120 min). The preparations were then centrifuged at 4°C for 10 min at 10,000 *g*, the supernatant was removed for scintillation counting, and 0.5 ml of PBS was added. The suspensions were mixed by vortexing, and the centrifugation step was repeated. The supernatant was removed and counted, and 0.5 ml of 50% ethanol was added to the pellets. The mixture was vortexed and removed, and a second 50% ethanol wash of the tube was added to this solution for counting as the plasma membrane fraction. A final 50% ethanol wash of the tubes determined that greater than 99% of the plasma membrane-associated radioactivity was recovered in the first two washes. Under this protocol, binding occurred at physiological body temperature. Thereafter, rapid packing of the membranes with subsequent cooling during centrifugation minimized redistribution of [^{3}H]OA between the plasma membranes, BSA, buffer, and the vessel walls prior to quantitation of isotope. The supernatants and plasma membrane fractions were counted by a dual label program. The first plasma membrane pellet contained ~4% of the BSA in the original incubation solution. Consistent with prior studies (50), the initial PBS wash removed half of this, but the remainder was essentially undiminished by further washes. Therefore the OA bound to the plasma membranes was corrected for this residual OA:BSA in the pellets. For this correction, the OA:BSA ratio of the bound complex was taken to be the same as that in the initial incubation medium, based on the recovery of both ^{14}C and ^{3}H in the pellets and supernatants of the wash/centrifugation steps. The OA bound to the BSA associated with the plasma membrane averaged 4% (and was always less than 8%) of the total bound OA in all samples. Subsequent cooling during centrifugation minimized redistribution of [^{3}H]OA from the plasma membranes to the solution and the walls of the tube.

OA initial uptake by suspended rat adipocytes

Suspensions of isolated adipocytes were prepared as described above from animals of the same age and weight as those used for the membrane-binding studies and were used immediately for studies of OA uptake. Initial uptake of [^{3}H]OA was measured by a rapid filtration technique described previously (7, 34). Ap-

Downloaded from www.jlr.org by guest, on June 14, 2012

proximately 1×10^6 cells in 100 μl of Dulbecco's modified Eagle's medium (DMEM) (51) were added to 240 μl of DMEM containing BSA and [^{3}H]OA at a BSA concentration of 500 μM and OA:BSA ratios of 0.05–6.0 and incubated for 0–30 s, a period during which cellular OA uptake is a linear function of time (34). At each specified time, uptake was stopped by addition of an ice-cold solution containing 0.1% BSA (a concentration that does not inhibit the action of phloretin and removes OA that adheres to the cell surface) and 200 μM phloretin (to inhibit the influx of further OA and the efflux of internalized OA) (8, 32, 34). The cells were then filtered and washed with the same solution. The filters were transferred to vials containing BCS scintillant (Amersham, Arlington Heights, IL), and cellular [^{3}H]OA content was quantitated by liquid scintillation spectroscopy. This protocol for measuring uptake derives from one initially introduced in 1981 (7), and has been used subsequently in numerous studies reported from many laboratories. Several specific aspects of the protocol contribute to the validity of the generated results. First, to avoid the confounding "albumin effects" on uptake observed at lower BSA concentrations, these studies were conducted at a BSA concentration of 500 μM. This is based on both experimental (52) and theoretical (53) evidence showing that, under these conditions, the rate of dissociation from albumin, pericellular unstirred layer effects, and "pseudofacilitation" make only vanishingly small contributions to the observed kinetics, which therefore accurately reflect transmembrane influx. Second, the use of this specific phloretin/BSA stop solution removed surface-bound OA and prevented its efflux from the cells (see Discussion). Finally, the volume of incubation medium relative to cells was chosen so that the concentration of [^{3}H]OA in the medium did not change appreciably during the period of incubation, and cell-associated radioactivity never exceeded 2% of the [^{3}H]OA in the initial incubation medium.

Cellular metabolism of fatty acids

Esterification of OA by adipocytes at 37°C was examined over the first 5 min of incubation with [^{3}H]OA, as described previously for hepatocytes (32, 54). Preliminary studies with [^{14}C]OA had previously shown that oxidation to $^{14}CO_2$ by adipocytes during this period was negligible. For these experiments, adipocyte OA uptake from solutions containing 250 μM OA and 500 μM BSA was stopped at various times from 0 to 5 min as described above. The washed adipocytes on the filters were extracted with chloroform-methanol and the lipids were separated by thin-layer chromatography (TLC). Identities of the lipid spots were determined by comparing their R_f values with those of commercial standards (54), after which the spots were cut out, extracted, and counted by scintillation spectroscopy. Total cellular [^{3}H]OA uptake was also measured over the same time period in duplicate samples.

Data analysis

Unbound OA concentrations in the presence of BSA were calculated from the successive association constants of Spector, Fletcher, and Ashbrook (46); Richieri, Anel, and Kleinfeld (47); Rose et al. (55); and the constants of Bojesen and Bojesen (56). [^{3}H]OA uptake and binding data were fitted to a variety of plausible functions of the calculated [OA_u], using a desktop computer version of the Simulation, Analysis, and Modeling (SAAM) program of Berman and Weiss (57). Details of the program and the data-fitting techniques involved have been described previously (57, 58). The rationale for the functions tested also has been described previously (45). Care was taken during the data-fitting process to find global rather than local minima in the sum of squares. If two models gave similarly optimal fits, the simpler of the two was used, because any added complexity only increases the uncertainty of the fitted parameters. In addition, published rates of entry of OA or palmitic acid into cells and vesicles (26, 28–31, 59) were corrected to 37°C (59) and the $t_{1/2}$ for fatty acid entry was plotted against the cell/vesicle diameter. These data were fitted to various smooth functions to establish a descriptive relationship. To estimate the rate constant for OA flip-flop (k_{ff}) into rat adipocytes from albumin-free incubation mixtures, we derived values for k_{ff} from the published data of Civelek et al. (29). In the best described study from that article, 130 nmol of OA was added to 1.3 ml of albumin-free incubation mixture containing isolated rat adipocytes (total [OA] = 100 μM, but actual [OA_u] indeterminate because of micelle formation and binding to vessel walls and membranes (29)) at 30°C, and subsequent deviations from the basal intracellular pH (pH_i) of 7.0, detected with an internalized indicator dye, were recorded. As values for k_{ff} were not reported by the authors, the published tracings of pH_i were scanned into computer files; individual data points were interpolated and analyzed using SAAM. The interpolated pH_i data were first used to generate curves of the actual intracellular concentrations of H^+ and OH^-. Changes in intracellular OH^- concentrations over the initial 240 s were fitted to several hypothetical statistical models.

RESULTS

OA binding and uptake by adipocytes

The shapes of the OA-binding and uptake curves observed in adipocytes are similar to those reported in hepatocytes (45), although the binding was measured over a wider range in the present study. OA binding and uptake were well described by simple functions of [OA_u], irrespective of whether the Spector, Fletcher, and Ashbrook (46) or Richieri, Anel, and Kleinfeld (47) OA:BSA association constants were used for the computation of the unbound ligand concentration. Using the Spector, Fletcher, and Ashbrook constants (46), both binding and uptake were best fitted by the sum of saturable and nonsaturable components (**Fig. 1A**) of the form

$$\text{Binding}([OA_u]) = \frac{B_{max}[OA_u]}{(K_d + [OA_u]) + k_b[OA_u]} \qquad \textit{Eq. 1)}$$

where B_{max} (picomoles of OA per 50,000 cells) is the maximum binding capacity of the saturable component, K_d is the unbound OA concentration at half-maximal binding (nanomolar), and k_b is the nonsaturable binding coefficient (microliters per 50,000 cells). For uptake, the analogous equation was

$$\text{Uptake } [OA_u] = \frac{V_{max}[OA_u]}{(K_m + [OA_u]) + k_n[OA_u]} \qquad \textit{Eq. 2)}$$

In this instance, V_{max} (picomoles of OA per 50,000 cells/s) and K_m (nanomolar) are, respectively, the maximal uptake rate of the saturable uptake component and the unbound OA concentration at half-maximal uptake velocity (nanomolar), and k_n (microliters per 50,000 cells per second) is the rate constant for nonsaturable uptake (45). The goodness of fit of the data to these equations is indicated by R^2 values for the binding and uptake fits of 0.994 and 0.999, respectively. Computed values for B_{max}, K_d, k_b, V_{max}, K_m, and k_n are presented in **Table 1**. By using the constants of

Downloaded from www.jlr.org by guest, on June 14, 2012

ASBMB JOURNAL OF LIPID RESEARCH

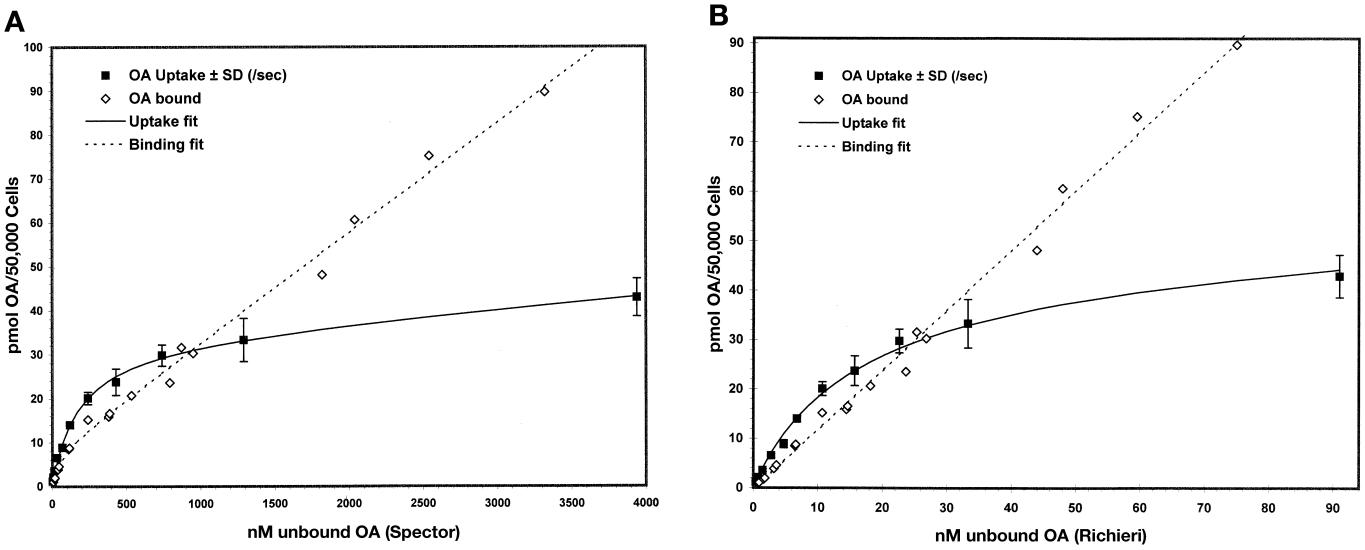

Fig. 1. The computer-fitted curves relating OA binding to adipocyte plasma membranes (open diamonds) and uptake by isolated adipocytes (solid squares) to calculated values for $[OA_u]$ over a range of OA:BSA molar ratios of 0-4. A: $[OA_u]$ calculated with the association constants of Spector, Fletcher, and Ashbrook (46). B: $[OA_u]$ calculated with the association constants of Richieri, Anel, and Kleinfeld (47). The uptake data are presented as means ± SD for triplicate determinations and the binding data are presented as individual determinations, accumulated over several days.

Richieri, Anel, and Kleinfeld (47) for calculation of $[OA_u]$, uptake was again best fitted by the sum of saturable and nonsaturable components according to equation 2, but binding was best described as a simple linear function of $[OA_u]$ (Fig. 1B). The R^2 values for the binding and uptake fits were also 0.994 and 0.999, respectively. Values for the calculated uptake and binding parameters are again presented in Table 1. On the basis of these parameter values, the saturable component of the curve describing adipocyte uptake of OA accounted for >90% of the total uptake at OA/BSA ratios ≤3.0; that is, in the normal physiologic range (**Fig. 2A**). The nonsaturable component contributed >50% only at $\nu > 5$ (Fig. 2B). This conclusion, similar to that reported for hepatocytes (45), was true regardless of whether the Spector or Richieri binding constants were used in the calculation of $[OA_u]$.

Rate constants for transmembrane movement of OA

Using the parameter values derived from the binding and uptake studies (Table 1) and the model developed with hepatocytes (45), the separate rate constants for the saturable (k_s) and nonsaturable (k_{ns}) transmembrane movement of OA into adipocytes can be calculated from the general relationship

$$k_x(\mathrm{s}^{-1}) = \frac{\mathrm{UT}_x\ (\mathrm{pmol}/50{,}000\ \mathrm{cells} \cdot \mathrm{s}^{-1})}{\mathrm{B}_x\ (\mathrm{pmol}/50{,}000\ \mathrm{cells})} \qquad \textit{Eq. 3)}$$

where k_x is the rate constant for component x, and UT_x and B_x are the relationships describing that component (i.e., saturable or nonsaturable) of uptake and binding as a function of $[OA_u]$. Using the constants of Spector, Fletcher, and Ashbrook (46) and assuming that the source of OA for saturable uptake is the OA bound saturably to

TABLE 1. Parameters of OA binding to rat adipocyte and hepatocyte plasma membranes and uptake by isolated rat adipocyte and hepatocyte suspension

	Binding			Uptake		
	B_{max}[a]	K_b[b]	k_b[c]	V_{max}[d]	K_m[e]	k_n[f]
Adipocytes						
Spector	9.3 ± 1.2	82 ± 15	24.8 ± 0.8	30.0 ± 1.7	115 ± 14	3.2 ± 0.5
Richieri	NA	NA	1,180 ± 30	44.0 ± 4.0	15.1 ± 1.6	62 ± 16
Hepatocytes						
Spector	5.6 ± 0.7	170 ± 30	9.6 ± 1.0	1.58 ± 0.14	153 ± 55	0.254 ± 0.008
Richieri	NA	NA	550 ± 20	2.78 ± 0.14	21.8 ± 2.7	4.2 ± 0.2

Abbreviation: NA, not applicable.
[a] B_{max}: pmol OA/50,000 cells.
[b] K_b: nM unbound OA.
[c] k_b: μl /50,000 cells.
[d] V_{max}: pmol OA/50,000 cells/s.
[e] K_m: nM unbound OA.
[f] k_n: μl /50,000 cells/s.

Downloaded from www.jlr.org by guest, on June 14, 2012

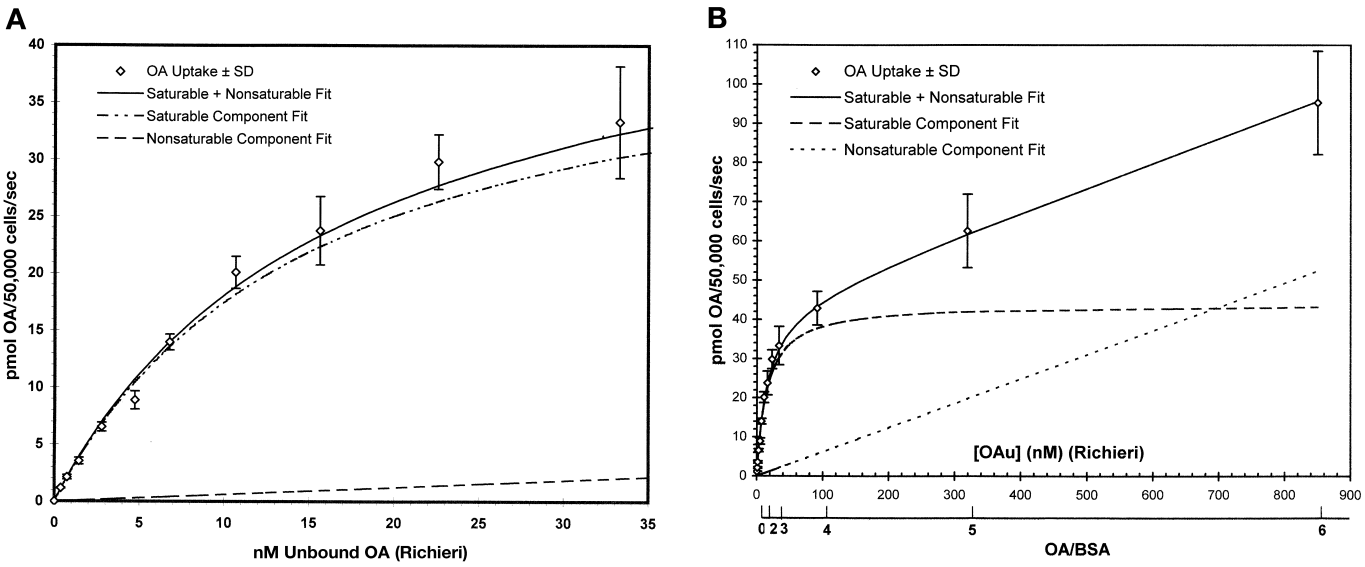

Fig. 2. The computer-fitted curve relating experimentally measured total OA uptake by isolated adipocytes (means ± SD, open diamonds) (solid line) and computer-generated saturable (dash-dot line) and nonsaturable (dotted line) uptake components, to values of $[OA_u]$ calculated with the OA:BSA association constants of Richieri, Anel, and Kleinfeld (47). A: OA:BSA range, 0–3. B: OA:BSA range, 0–6.

the plasma membrane and that for nonsaturable uptake is the OA bound nonsaturably to the membrane, the rate constant for saturable uptake is given by

$$k_s = \frac{V_{max}/(K_m + [OA_u])}{B_{max}/(K_b + [OA_u])} \qquad \textit{Eq. 4)}$$

For $[OA_u]$ within the physiologic range ($\nu = 0.5$–3), $k_s = 2.4 \pm 0.6$ to $3.3 \pm 0.5\ s^{-1}$ ($t_{1/2} = 0.29 \pm 0.08$ to 0.21 ± 0.03 s); at the midpoint of this range ($\nu = 1.5$), $k_s = 2.9 \pm 0.4\ s^{-1}$ ($t_{1/2} = 0.24 \pm 0.04$ s). Similarly, under the assumption that one-half of the OA bound nonsaturably to the plasma membrane in these experiments is bound to the outer leaflet (45), the rate constant for nonsaturable OA transfer across the plasma membrane is given by

$$k_{ns} = \frac{2k_n}{k_b} \qquad \textit{Eq. 5)}$$

Accordingly, $k_{ns} = 0.26 \pm 0.04\ s^{-1}$ ($t_{1/2} = 2.7 \pm 0.4$ s). A similar analysis using parameter values calculated on the basis of the constants of Richieri, Anel, and Kleinfeld (47) is more complicated. Because the binding curve is a linear function of $[OA_u]$, either OA is saturably bound to the plasma membrane in amounts that are undetectably small compared with the nonsaturably bound OA or saturable and nonsaturable uptake both derive from the same nonsaturably bound OA pool. If the former is the case, the saturable rate constant is fast ($k_s > 25\ s^{-1}$), whereas if the latter is true, the saturable rate constant ranges from $4.9 \pm 1.1\ s^{-1}$ at $[OA_u] \sim 0$ to a value of 0 as $[OA_u]$ approaches infinity. Within the normal physiologic range (OA:BSA = 0.5–3), $k_s = 4.2 \pm 0.9$ to $1.5 \pm 0.3\ s^{-1}$ ($t_{1/2} = 0.16 \pm 0.03$ to 0.45 ± 0.10 s); at the midpoint of this range ($\nu = 1.5$), $k_s = 2.9 \pm 0.3\ s^{-1}$ ($t_{1/2} = 0.24 \pm 0.03$ s). The nonsaturable rate constant $k_{ns} = 0.104 \pm 0.028\ s^{-1}$ ($t_{1/2} = 6.6 \pm 1.7$ s) at all $[OA_u]$. The similarities in the values of k_s and k_{ns} calculated with $[OA_u]$ that differ by 1–2 orders of magnitude reflect, in part, the fact that both $[OA_u]$ and/or parameters derived from them appear in both the numerator and denominator of equations 4 and 5.

Recalculation with the constants of Richieri, Anel, and Kleinfeld (47) of our previous data describing OA binding and uptake in hepatocytes (45) yields similar results. The best fit of the uptake data remains a combination of saturable and nonsaturable functions, but OA binding to plasma membranes was best described by a simple linear relationship (Table 1). Nevertheless, using either set of OA:BSA association constants taken from Table 1, the calculated value for k_s is ~15 times k_{ns}.

Adipocyte metabolism of OA

After uptake, the metabolism of OA by adipocytes was rapid (**Fig. 3A**). TLC of cellular extracts demonstrated that, within the 1–2 s required to chill and wash the cells, 18% of the [^{3}H]OA in the initial, 0 time sample had already been esterified. By 15 and 30 s, 72% and 83%, respectively, was esterified, and this increased progressively to 95% at 5 min. When corrected for the recovery of standards, recovery of [^{3}H]OA and its esters from the TLC plates averaged 96% of total cell-associated radioactivity. These data confirm prior evidence (32, 34, 35) that our experimental protocol measures true cellular uptake and that the [^{3}H]OA measured as being taken up rapidly enters cellular metabolic pathways. The amount of free [^{3}H]OA in the cells remained essentially constant after the first 15 s, while that of each of the esters gradually rose (Fig. 3B). The pattern of esters observed over time suggests that [^{3}H]OA was converted first to monotriglycerides and then sequentially to di- and triglycerides. Analogous data have been obtained in hepatocytes, although esterification in that setting proceeds more slowly (32,

Downloaded from www.jlr.org by guest, on June 14, 2012

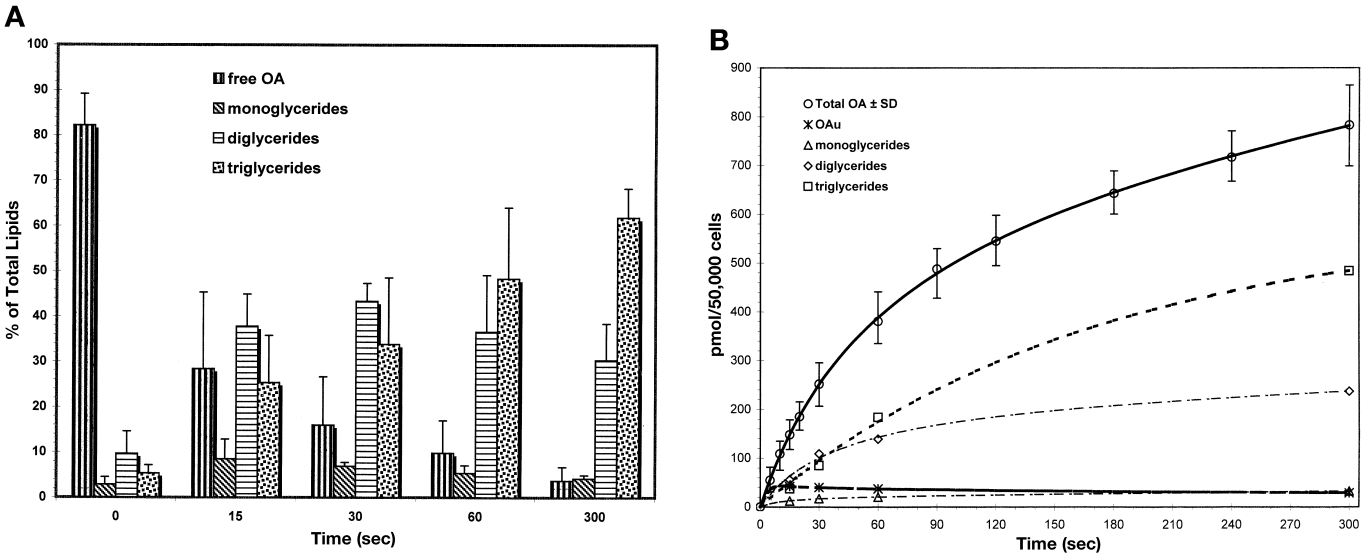

Fig. 3. A: The relative proportions of unesterified [^{3}H]OA and its tritiated mono-, di-, and triglyceride esters in extracts from adipocytes at 0, 15, 30, 60, and 300 s during the incubation of adipocyte cell suspensions in 250 μM OA:500 μM BSA at 37°C. At the indicated time of incubation, a further 1–2 s was required to stop uptake and metabolism prior to lipid extraction. The values represent means ± SE. B: Total OA uptake by rat adipocytes at 37°C from 0 to 300 s and the calculated concentrations of free OA and its esters.

58). By contrast, in studies at high, nonphysiologic values for [OA_u], the majority of the uLCFA taken up by adipocytes do not enter normal metabolic compartments, because ≥50% of OA taken up remained available for efflux and was therefore nonesterified, after 4 min (29).

DISCUSSION

The data presented above provide important information about the processes by which cells take up uLCFA. Some of this information represents a significant confirmation of observations reported earlier, whereas other data offer entirely new insights. Thus, the existence of both saturable and nonsaturable OA uptake mechanisms in adipocytes and cardiac myocytes could be inferred from studies of OA uptake kinetics published in 1988 (34, 35). Similar dual pathways for uLCFA uptake by hepatocytes were explicitly described in a 1992 study that also presented a model for calculating transmembrane rate constants for uptake of OA by each of these pathways from simultaneous determinations of OA uptake kinetics and its binding to plasma membranes (45). A direct comparison of k_{ns} and k_{ff}, measured in the same cell type, has not previously been reported.

The results reported in this study depend critically on the validity of the technique used for measuring cellular uLCFA uptake. This, in turn, requires that the experimental measurements of cell-associated radioactivity accurately reflect total cellular uptake, avoiding any appreciable loss of radioactivity by efflux from cells during processing. The use of cold stop solutions containing phloretin to achieve this purpose was first described by Abumrad, Park, and Park (8), whose data in isolated rat adipocytes clearly indicated that phloretin "stopped" the transmembrane movement of uLCFA either into or from the cell. In these studies, the incorporation of BSA in the stop solution at concentrations in excess of 0.1% was reported to interfere with the phloretin effect, and was not pursued. In subsequent work by Stremmel and Berk (32) in isolated rat hepatocytes and Schwieterman et al. (34) in adipocytes, the following observations were reported: *i*) A stop solution of 200 μM phloretin in cold PBS blocked the efflux of labeled uLCFA during sample processing that had been observed with PBS alone; *ii*) a stop solution of BSA in cold PBS resulted in the virtually instantaneous removal of ~50% of cell-associated radioactivity, followed by a slower further loss, the rate and extent of which depended on the BSA concentration; and *iii*) a stop solution of 200 μM phloretin/0.1% BSA in cold PBS again led to the virtually instantaneous removal of ~50% of cell-associated radioactivity, after which levels remained constant. These experiments were interpreted as indicating that the phloretin in the stop solution inhibited both influx and efflux of labeled uLCFA from the cells under study, while the BSA removed uLCFA that was merely adherent to the cell surface but not internalized. Subsequently, cold phloretin/BSA stop solutions have been widely used, as described in publications from several laboratories studying uLCFA uptake by a variety of cell types (60, 61).

Nevertheless, the exact mechanism by which phloretin affects cellular uLCFA uptake is unclear. Its adsorption to both biological and artificial membranes results in altered membrane permeability for a variety of charged and neutral compounds (62). Several aspects of this phenomenon have been studied in some detail. Phloretin and its analogues alter the dipole potential of lipid bilayers, decreasing transmembrane anion fluxes while increasing the flux of cations (63). This apparently occurs by the vectoral interaction of particular phloretin conformers (64), thereby

Downloaded from www.jlr.org by guest, on June 14, 2012

reducing the inherent dipole potential of the membrane. Second, phloretin strongly decreases the lipid-phase transition temperature (64), a property that can affect any transmembrane movement. It also appears to affect lipid packing, but the relation between surface potential change and lipid packing is not simple (62). Finally, while phloretin binds nonspecifically to membranes by interacting with the phospholipid head groups (64), it also binds specifically to certain proteins, including some transport proteins (65), the transport function of which it inhibits (66). Which of these mechanisms is important in preventing uLCFA efflux is unknown, but the evidence that phloretin inhibits virtually 100% of uLCFA efflux from hepatocytes and adipocytes is quite clear.

Despite both kinetic evidence and the identification of several plasma membrane proteins as putative uLCFA transporters (9–15), several studies have continued to argue that cellular OA uptake occurs exclusively by passive flip-flop across the lipid bilayer of the plasma membrane (see 16, 18, and 21 for reviews). Because apparent flip-flop rates for entry of natural uLCFA into small unilamellar vesicles of ~200 Å in diameter are extremely rapid ($k_{ff} >$ 200 s^{-1}), it was argued that there was no physiologic role for an alternative uLCFA uptake mechanism (26). However, studies of large (26, 28) or giant unilamellar vesicles (28) of ~1,000 and ≥2,000 Å found progressively smaller values for k_{ff} (3–15 and 0.1–1.0 s^{-1}, respectively), and flip-flop rates reported in red blood cell ghosts were similar to those determined in giant unilamellar vesicles (59). The magnitude of k_{ff} varied with vesicle composition (in particular decreasing with increasing cholesterol content, particularly at low temperatures) and decreased with increasing vesicle size (reviewed in 17 and 23). For vesicles most closely approaching the size and lipid composition of cell membranes, reported flip-flop $t_{1/2}$ values for uLCFA such as OA and palmitate were in the range of 1–10 s (17, 28, 59). Although this has also been debated, the most recent data indicate that flip-flop is the rate-limiting step in the passive transmembrane movement of protonated uLCFA into vesicles (28, 59, 67). These data are especially compelling in giant vesicles and RBC ghosts, which most closely resemble the sizes of viable cells (59).

Because uptake of protonated uLCFA is followed by ionization of the carboxyl group and intracellular acidification, several of the studies cited above have attempted to use changes in pH_i to estimate rates of uLCFA entry into both vesicles (24–26), and adipocytes, pancreatic β cells, and cytotoxic T lymphocytes (29–31). Our analysis of the data of Civelek et al. (29), which describe the rate of change of pH_i during OA uptake by adipocytes at 30°C, indicates that the observed changes in H^+ and OH^- concentrations after addition of OA are well described by a sum of two exponential components, with $t_{1/2}$ values of 6 and ~100 s. Even the rapid initial component (k_1 = 0.114 s^{-1}, $t_{1/2}$ = 6.1 s) is much slower than the estimated $t_{1/2}$ for the facilitated (saturable) transfer of uLCFA across hepatocyte (k_s = 0.7 s^{-1}) (45) and adipocyte (k_s 2.4 s^{-1}; see above) plasma membranes. Because the change in pH_i in a similar experiment in pancreatic β-cells exhibited only a single exponential with a $t_{1/2}$ of 60 s (30), we initially considered the slower component to reflect the rate of transmembrane OA flip-flop (45). However, the effects on pH_i of inhibiting Na^+/H^+ exchange with 5-(*N*-ethyl, *N*-isopropyl)-amiloride (29) suggest that it is the rapid component that reflects the initial entry rate of the protonated uLCFA (k_{ff}). The slower exponential component is most consistent with modification of the rate of uLCFA-induced changes in pH_i brought about by activation of the plasma membrane Na^+/H^+ exchanger. The value for k_1, corrected to 37°C, is 0.16 ± 0.02 s^{-1} ($t_{1/2}$ = 4.3 ± 0.5 s), and is similar to the values for k_{ns} in adipocytes, described above. The close agreement between values of k_{ns} and k_1, obtained by widely differing methods, suggests they are both measures of the same process. Thus, the available data, representing the first effort to compare flip-flop rates with parameters measured under more physiologic conditions, indicate that the $t_{1/2}$ for passive flip-flop of uLCFA into living adipocytes is 2.7–6.6 s, whether estimated from changes in pH_i or by tracer methods. This is precisely the range predicted from an examination of the relationship between vesicle/cell diameter and k_{ff} reported in earlier studies (26, 28–31, 59). Indeed, k_1 and k_{ns} are both highly correlated with flip-flop rates reported in synthetic vesicles of various sizes and in red cell ghosts (r = 0.93) (**Fig. 4**).

The data presented above indicate that there are two distinct modes of entry of OA into adipocytes: a saturable process that moves OA across the plasma membrane with a rate constant k_s of at least 2.9 s^{-1} ($t_{1/2}$ = 0.24 s) and a nonsaturable process approximately an order of magnitude slower, with a rate constant k_{ns} = 0.10–0.26 s^{-1} ($t_{1/2}$ =

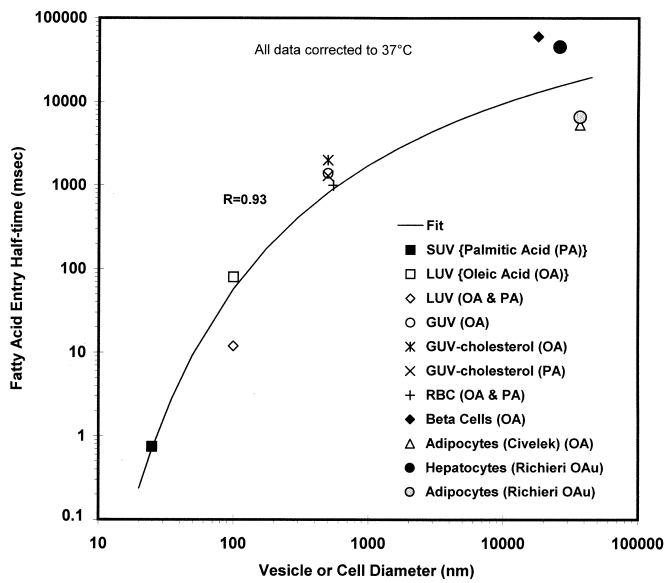

Fig. 4. The $t_{1/2}$ of nonfacilitated OA entry into cells and vesicles, expressed as a function of mean cell or vesicle diameter. The data from the existing literature (see text) have been corrected to 37°C where necessary, using the temperature dependence determined by Kleinfeld et al. (59). The fitted line is a hyperbolic function used for descriptive purposes to illustrate the trend. SUV, Small unilamellar vesicles; LUV, large unilamellar vesicles; GUV, giant unilamellar vesicles; RBC, red blood cells; OAu, unbound OA uptake.

Downloaded from www.jlr.org by guest, on June 14, 2012

2.7–6.6 s). This central conclusion is arrived at irrespective of whether the values of $[OA_u]$ required for the computation of k_s and k_{ns} are calculated from the OA:BSA association constants of Spector, Fletcher, and Ashbrook (46), or the more recent values of Richieri, Anel, and Kleinfeld (47), from which the estimates of $[OA_u]$ are at least 10-fold lower. Hence, this conclusion is largely independent of the particular OA:BSA association constants used.

The tracer kinetic studies presented above indicate that the saturable uptake component is the predominant pathway for adipocyte uLCFA uptake at the low $[OA_u]$ that occur with physiologic albumin concentrations and ν values ($\nu \leqslant 3$). These conditions reflect the typical state in plasma in a well-fed mammal between meals. As ν increases beyond this range, nonsaturable uptake becomes increasingly important, exceeding 50% of uptake at $\nu > 5.8$, at which $[OA_u]$, computed according to Richieri, Anel, and Kleinfeld (47), is ~0.7 μM. The flip-flop studies of Civelek et al. (29) used a total OA concentration of 100 μM without albumin, yielding a high but indeterminate $[OA_u]$. These are precisely the conditions under which the nonsaturable component would be expected to dominate overall uptake to a degree that would make the saturable process undetectable. In short, like the blind men and the elephant, what is seen to be the dominant uLCFA uptake process depends highly on which end of the spectrum of $[OA_u]$ values is used in the studies. Given the differences in the methods used, the similarities in the value of k_{ns} and k_{ff} suggest that they both measure the same process.

Although we believe that the conditions under which typical "flip-flop" studies (26, 28–31) were conducted preclude the recognition of an important, saturable process involved in cellular uLCFA uptake, they do provide convincing evidence that the passive, flip-flop process reflects the transmembrane movement of protonated uLCFA. By contrast, it appears likely that the saturable process is responsible for transfer of negatively charged uLCFA anions across the plasma membrane. Studies by Gutknecht (68), as well as more recent reports by Schmider et al. (69), indicate that the purely passive transmembrane flip-flop of long chain fatty acid anions is slow. Moreover, the hepatocellular uptake kinetics of $\alpha_2,\beta_2,\omega_3$-heptafluoro-[^{3}H]stearate (HFS), a highly acidic ($pK_a = 0.5$) uLCFA analogue that exists almost exclusively as an anion at physiologic pH, are virtually identical to those of natural stearate at unbound ligand concentrations at which >90% of uptake is saturable (70). In addition, uptake of both stearate and [^{3}H]HFS was inhibited to a similar degree by prior photoaffinity labeling of the cell surface with 11,11-azistearate (71) and by preincubation with an antibody to a putative uLCFA transporter, plasma membrane fatty acid-binding protein (S-L. Zhou and P. D. Berk, unpublished). That the saturable uLCFA uptake component reflects transport of fatty acid anions is further supported by reports that the saturable component of uLCFA uptake is inhibited by 4,4′-diisothiocyanostilbene-2,2′-disulfonate and other inhibitors of anion transport (reviewed in 22), and by recognition that uncoupling protein facilitates H^+ import into the mitochondrial matrix by transporting uLCFA anions across the inner mitochondrial membrane from the matrix to the intramembranous space, where they associate with a proton. The resulting protonated species diffuse passively down a concentration gradient back to the matrix (72–74). On the basis of these and other observations, for example, of the effects on cellular uLCFA uptake kinetics of the expression of putative transporter cDNAs or of preincubation with antibodies to these proteins (20, 22, 23, 75), our working model of cellular uLCFA uptake is one in which uLCFA uptake occurs by two distinct processes: rapid, protein-mediated transport of uLCFA anions and the slower passive flip-flop of protonated uLCFA across the lipid bilayer.

An additional important result of the current studies is a better understanding of the impact of using particular OA:BSA association constants to compute $[OA_u]$ on the interpretation of OA binding and uptake studies. Constants determined by Spector, Fletcher, and Ashbrook in 1971 (46) were long the only ones sufficiently detailed to use over a wide range of uLCFA:BSA molar ratios. More recently several investigators (47, 55, 56) have reported new values for these constants. There seems to be general agreement that the Spector, Fletcher, and Ashbrook values give $[OA_u]$ values that are too high, by 1–2 orders of magnitude, and the impact of these different association constants on the interpretation of uLCFA uptake and binding data has been questioned (16) but not systematically studied heretofore. Because, consistent with standard pharmacokinetic theory, experimentally measured values of both binding and uptake are conventionally described as functions of $[OA_u]$, a lower computed value of $[OA_u]$ at a given ν would require a correspondingly higher functional "multiplier effect" affecting the binding or uptake constants at that ν. The higher "multiplier" would not change the nature of the function relating binding or uptake to $[OA_u]$ if it were relatively constant over a range of values for ν. However, if different sets of association constants result in differences not only in the absolute magnitude of particular computed values for $[OA_u]$ but also in the shape of the function relating $[OA_u]$ to ν, then the apparent functional relationship between $[OA_u]$ and measured values of uptake and binding may be altered. The most detailed of the more recently determined OA:BSA association constants are those of Richieri, Anel, and Kleinfeld (47), which are in close agreement with those of Rose et al. (55), determined by an entirely different method. A third set of constants, reported by Bojesen and Bojesen (56), yields unbound uLCFA concentrations that are still lower by another order of magnitude, but is less well characterized over the physiologically realizable range of ν, and does not use successive association constants to calculate unbound uLCFA. For all four published sets of association constants, calculated values for $[OA_u]$ increase linearly with ν for $\nu < 0.25$ (**Fig. 5A**). However, starting at $\nu \sim 0.25$, the $[OA_u]$ calculated from the constants of Spector, Fletcher, and Ashbrook (46) increase progressively more rapidly with increasing ν than those computed with the constants of Richieri, Anel, and Kleinfeld (47), Rose et al. (55), or Bojesen and Bojesen (56).

Downloaded from www.jlr.org by guest, on June 14, 2012

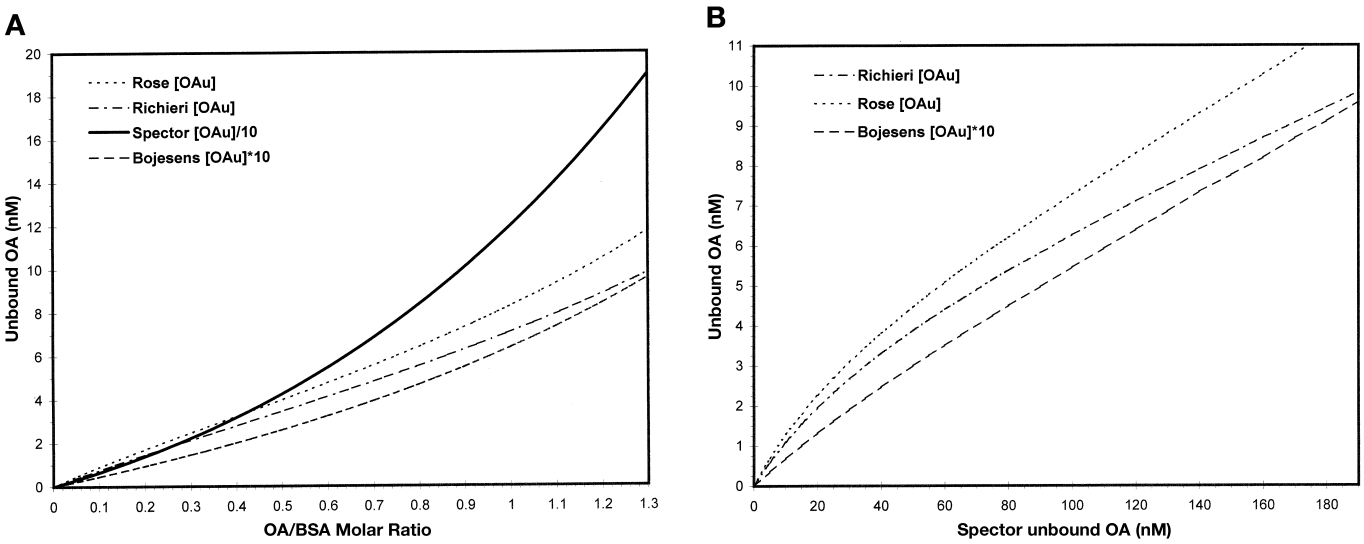

Fig. 5. $[OA_u]$ calculated from the association constants of Richieri et al. (dash-dot line), Rose et al. (dotted line), Bojesen and Bojesen (dashed line), and Spector et al. (solid line). A: All four sets of $[OA_u]$ plotted against the OA:BSA ratio in the range $\nu = 0–1.4$. Concentrations calculated according to Spector are divided by 10 and those according to Bojesen and Bojesen are multiplied by 10 for comparison of the slopes. B: $[OA_u]$ calculated with the binding constants of Richieri et al., Rose et al., and Bojesen and Bojesen, plotted as functions of the $[OA_u]$ calculated according to Spector et al.

Consequently, when $[OA_u]$ calculated from any of these alternative sets of constants are plotted as functions of the $[OA_u]$ calculated from the Spector, Fletcher, and Ashbrook constants at the same values for ν (Fig. 5B), the curves seem to contain a saturable component. Thus, any results that are linear with respect to, for example, the values of Richieri, Anel, and Kleinfeld (47) for $[OA_u]$ will exhibit a saturable component when plotted against those of Spector, Fletcher, and Ashbrook (46). If the OA:BSA association constants of Richieri, Anel, and Kleinfeld are closer to the "true" values, using the constants of Spector, Fletcher, and Ashbrook could give the appearance of saturability to a relationship between $[OA_u]$ and either binding or uptake that is actually linear.

In reviewing studies from our laboratory over two decades that used the Spector, Fletcher, and Ashbrook association constants, we found several instances of this phenomenon. Use of the Spector, Fletcher, and Ashbrook constants appears to be responsible for the apparent saturable component in the binding of OA to adipocyte plasma membranes reported above, and also in the binding of OA to both native and heat-denatured hepatocyte plasma membranes (45). The latter data were published before the constants of Richieri, Anel, and Kleinfeld were reported. When these binding data for liver plasma membranes were reanalyzed using $[OA_u]$ values calculated from the OA:BSA association constants of Richieri, Anel, and Kleinfeld (47), OA binding to both native and heat-denatured membranes was a linear function of $[OA_u]$ ($R^2 = 0.987$ and 0.997, respectively) (Table 1). If the Spector, Fletcher, and Ashbrook constants (46) were used in the calculation of $[OA_u]$, both these curves were best fitted by the sum of a saturable and a nonsaturable component (45). In fact, all of our studies of OA binding to plasma membranes give excellent linear fits when plotted against $[OA_u]$ calculated with the association constants of Richieri, Anel, and Kleinfeld, but exhibit apparent saturable components when plotted against $[OA_u]$ calculated with the Spector, Fletcher, and Ashbrook constants. The same is true for the uptake of OA by 3T3-L1 fibroblasts, which was reported to exhibit a small saturable component (41), but is linear with respect to $[OA_u]$ calculated according to Richieri, Anel, and Kleinfeld ($R^2 = 0.998$). However, this is not the case for studies of OA uptake by 4-day or 8-day 3T3-L1 adipocytes in that study (data not shown). Indeed, the functions relating cellular OA uptake to $[OA_u]$ for hepatocytes, cardiac myocytes, jejunal enterocytes, and 3T3-L1 and rat and mouse adipocytes (32–36, 39, 41, 51, 76) are predominantly saturable over the physiologic range of ν values regardless of the OA:BSA association constants used to calculate $[OA_u]$. Although the ADIFAB (Molecular Probes, Eugene, OR) method used by Richieri, Anel, and Kleinfeld (47) to determine OA:BSA association constants is not free of criticism (77), the excellent linear fits of all three sets of data for OA binding to plasma membranes (including heat-denatured hepatocyte membranes) with respect to the $[OA_u]$ of Richieri, Anel, and Kleinfeld lend some credence to those values. The probability of this occurring by chance seems small. It must be emphasized, however, that it is not the magnitudes of the computed $[OA_u]$ but the functional relationship of $[OA_u]$ to ν that influences the physiologic interpretation of experimental uptake and binding data.

Current studies suggest that the nonsaturable uLCFA uptake process is quantitatively important only at high uLCFA: albumin ratios not commonly achieved in bulk plasma. Thus, cell-specific modulation of facilitated uLCFA uptake may provide a mechanism for regulating substrate parti-

Downloaded from www.jlr.org by guest, on June 14, 2012

tioning under basal conditions. However, the lipolytic action of lipoprotein lipase (LPL) located on the lumenal surface of the vascular endothelium, and of hormone-sensitive lipase (HSL) within adipocytes, may rapidly generate high, local concentrations of nonesterified uLCFA. To the best of our knowledge, the actual local uLCFA concentrations involved have not been measured. However, it is conceivable, even likely, that under the influence of these enzymes, passive flip-flop of the resulting uLCFA temporarily becomes the major route of transmembrane uLCFA flow across capillary endothelium and into parenchymal cells under the influence of LPL, and out of cells (especially adipocytes) under the influence of HSL. Up-regulation of protein-mediated transport systems typically requires a finite time delay for either the synthesis of additional molecules of transport proteins or, for example, in the case of glucose transporter 4 and of the uLCFA fatty acid transporter/CD36 in skeletal muscle (78), the insertion of preexisting pools of such proteins into the plasma membrane. However, passive flip-flop across cell membranes may provide a mechanism for responding virtually instantaneously to marked local changes in the concentration of uLCFA. The constant availability of this mechanism would be a particular advantage because accumulation of high concentrations of uLCFA intracellularly, for example, during active lipolysis, can be highly toxic.

Ultimately, the significance of facilitated uLCFA transport systems lies in the roles these systems play in human physiology, pathophysiology, and disease. Cell-specific changes in the V_{max} for saturable OA uptake occur in animal models of a number of human disease states, including obesity, type 2 diabetes, alcoholic liver disease, and cardiomyopathy, often in parallel with altered expression of one or more of the putative uLCFA transporters (41, 51, 76, 79–81). In addition, a report attributes a syndrome of recurrent episodes of severe liver failure in children to a membrane defect in uLCFA transport (82). Failure to consider carefully the likely existence of facilitated transport processes for cellular uLCFA uptake will impair the ability to apply the results of basic studies of membrane transport to the understanding of human physiology and disease.

This work was supported by grants DK-26438 and DK-52-401 from the National Institute of Diabetes, Digestive and Kidney Diseases of the National Institutes of Health and the Liver Disease Research Fund.

Manuscript received 16 August 2000, in revised form 17 October 2000, and in re-revised form 21 November 2000.

REFERENCES

1. Distel, R. J., G. S. Robinson, and B. M. Spiegelman. 1992. Fatty acid regulation of gene expression. *J. Biol. Chem.* **267:** 5937–5941.
2. Bernlohr, D. A., N. R. Coe, M. A. Simpson, and A. V. Hertzel. 1997. Regulation of gene expression in adipose cells by polyunsaturated fatty acids. *Adv. Exp. Med. Biol.* **422:** 145–156.
3. Sfeir, Z., A. Ibrahimi, E. Amri, P. Grimaldi, and N. Abumrad. 1997. Regulation of FAT/CD36 gene expression: further evidence in support of a role of the protein in fatty acid binding/transport. *Prostaglandins Leukot. Essent. Fatty Acids.* **57:** 17–21.
4. Grimaldi, P. A., L. Treboul, D. Gaillard, A. V. Armengod, and E. Z. Amri. 1999. Long chain fatty acids as modulators of gene transcription in preadipocyte cells. *Mol. Cell. Biochem.* **192:** 63–68.
5. McGarry, J. D. 1994. Disordered metabolism in diabetes: have we underemphasized the fat component? *J. Cell Biochem.* **55S:** 29–38.
6. Björntorp, P. 1994. Fatty acids, hyperinsulinemia, and insulin resistance: which comes first? *Curr. Opin. Lipidol.* **5:** 166–174.
7. Abumrad, N. A., R. C. Perkins, J. H. Park, and C. R. Park. 1981. Mechanism of long chain fatty acid permeation in the isolated adipocyte. *J. Biol. Chem.* **256:** 9183–9191.
8. Abumrad, N. A., J. H. Park, and C. R. Park. 1984. Permeation of long-chain fatty acid into adipocytes. *J. Biol. Chem.* **259:** 8945–8953.
9. Stremmel, W., G. Strohmeyer, F. Borchard, S. Kochwa, and P. D. Berk. 1985. Isolation and partial characterization of a fatty acid binding protein in rat liver plasma membranes. *Proc. Natl. Acad. Sci. USA.* **82:** 4–8.
10. Abumrad, N. A., M. Raafat El-Maghrabi, E-Z. Amri, E. Lopez, and P. A. Grimaldi. 1993. Cloning of a rat adipocyte membrane protein implicated in binding or transport of long-chain fatty acids that is induced during preadipocyte differentiation. *J. Biol. Chem.* **268:** 17665–17668.
11. Schaffer, J. E., and H. F. Lodish. 1994. Expression cloning and characterization of a novel adipocyte long chain fatty acid transport protein. *Cell.* **79:** 427–436.
12. Hirsch, D., A. Stahl, and H. F. Lodish. 1998. A family of fatty acid transporters conserved from mycobacterium to man. *Proc. Natl. Acad. Sci. USA.* **95:** 8625–8629.
13. Stahl, A., D. J. Hirsch, R. E. Gimeno, S. Punreddy, P. Ge, N. Watson, S. Patel, M. Kotler, A. Raimondi, L. A. Tartaglia, and H. F. Lodish. 1999. Identification of the major intestinal fatty acid transport protein. *Mol. Cell.* **4:** 299–308.
14. Trigatti, B. L., D. Mangaroo, and G. E. Gerber. 1991. Photoaffinity labeling and fatty acid permutation in 3T3-L1 adipocytes. *J. Biol. Chem.* **266:** 22621–22625.
15. Fujii, S., H. Kawaguchi, and H. Yasuda. 1987. Isolation and partial characterization of an amphiphilic 56-kDa fatty acid binding protein from rat renal basolateral membrane. *J. Biochem. Biophys. Res.* **101:** 679–684.
16. Hamilton, J. A., and F. Kamp. 1999. How are free fatty acids transported in membranes? Is it by proteins or free diffusion through the lipids? *Diabetes.* **48:** 2255–2269.
17. Kleinfeld, A. M. 2000. Lipid phase fatty acid flip-flop: is it fast enough for cellular transport? *J. Membr. Biol.* **175:** 79–86.
18. Noy, N., and D. Zakim. 1993. Physical chemical basis for the uptake of organic compounds by cells. *In* Hepatic Transport and Bile Secretion. N. Tavoloni and P. D. Berk, editors. Raven Press, New York. 313–335.
19. Kleinfeld, A. M. 1995. Fatty acid transport across membranes. *In* Stability and Permeability of Lipid Bilayers. E. A. Disalvo and S. Simon, editors. CRC Press, Boca Raton, FL. 241–258.
20. Glatz, J. F. C., J. F. P. Luiken, F. A. Van Nieuwenhoven, and G. J. Van der Vusse. 1997. Molecular mechanism of cellular uptake and intracellular translocation of fatty acids. *Prostaglandins Leukot. Essent. Fatty Acids.* **57:** 3–9.
21. Hamilton, J. A. 1998. Fatty acid transport: difficult or easy? *J. Lipid Res.* **39:** 467–481.
22. Abumrad, N., C. Harmon, and A. Ibrahimi. 1998. Membrane transport of long-chain fatty acids: evidence for a facilitated process. *J. Lipid Res.* **39:** 2309–2318.
23. Berk, P. D., and D. D. Stump. 1999. Mechanisms of cellular uptake of long chain free fatty acids. *Mol. Cell. Biochem.* **192:** 17–31.
24. Kamp, F., and J. A. Hamilton. 1992. pH gradients across phospholipid membranes caused by fast flip-flop of un-ionized fatty acids. *Proc. Natl. Acad. Sci. USA.* **89:** 11367–11370.
25. Kamp, F., H. V. Westerhoff, and J. A. Hamilton. 1993. Movement of fatty acids, fatty acid analogues, and bile acids across a phospholipid bilayer. *Biochemistry.* **32:** 11074–11086.
26. Kamp, F., D. Zakim, F. Zhang, N. Noy, and J. A. Hamilton. 1995. Fatty acid flip-flop in phospholipid bilayers is extremely fast. *Biochemistry.* **34:** 11928–11937.
27. Daniels, C., N. Noy, and D. Zakim. 1985. Rates of hydration of fatty acids bound to unilamellar vesicles of phosphatidylcholine or to albumin. *Biochemistry.* **24:** 3286–3292.
28. Kleinfeld, A. M., P. Chu, and C. Romero. 1997. Transport of long chain native fatty acids across lipid bilayer membranes indicates that transbilayer flip-flop is rate limiting. *Biochemistry.* **36:** 14146–14158.

Downloaded from www.jlr.org by guest, on June 14, 2012

29. Civelek, V. N., J. A. Hamilton, K. Tornheim, K. L. Kelly, and B. E. Corkey. 1996. Intracellular pH in adipocytes: effects of free fatty acid diffusion across the plasma membrane, lipolytic agonists, and insulin. *Proc. Natl. Acad. Sci. USA.* **93:** 10139–10144.
30. Hamilton, J. A., V. N. Civelek, F. Kamp, K. Tornheim, and B. E. Corkey. 1994. Changes in internal pH caused by movement of fatty acids into and out of clonal pancreatic beta-cells (HIT). *J. Biol. Chem.* **269:** 20852–20856.
31. Richieri, G. V., and A. M. Kleinfeld. 1989. Free fatty acid perturbation of transmembrane signaling in cytotoxic T lymphocytes. *J. Immunol.* **143:** 2302–2310.
32. Stremmel, W., and P. D. Berk. 1986. Hepatocellular influx of [^{14}C]oleate reflects membrane transport rather than intracellular metabolism or binding. *Proc. Natl. Acad. Sci. USA.* **83:** 3086–3090.
33. Stremmel, W., G. Strohmeyer, and P. D. Berk. 1986. Hepatocellular uptake of oleate is energy dependent, sodium linked, and inhibited by an antibody to a hepatocyte plasma membrane fatty acid binding protein. *Proc. Natl. Acad. Sci. USA.* **83:** 3584–3588.
34. Schwieterman, W., D. Sorrentino, B. J. Potter, J. Rand, C-L. Kiang, D. Stump, and P. B. Berk. 1988. Uptake of oleate by isolated rat adipocytes is mediated by a 40-kDa plasma membrane fatty acid binding protein closely related to that in liver and gut. *Proc. Natl. Acad. Sci. USA.* **85:** 359–363.
35. Sorrentino, D., D. Stump, B. J. Potter, R. B. Robinson, R. White, C-L. Kiang, and P. D. Berk. 1988. Oleate uptake by cardiac myocytes is carrier mediated and involves a 40-kD plasma membrane fatty acid binding protein similar to that in liver, adipose tissue and gut. *J. Clin. Invest.* **82:** 928–935.
36. Stremmel, W. 1988. Fatty acid uptake by isolated rat heart myocytes represents a carrier-mediated transport process. *J. Clin. Invest.* **81:** 844–852.
37. Turcotte, L. P., B. Kiens, and E. A. Richter. 1991. Saturation kinetics of palmitate uptake in skeletal muscle. *FEBS Lett.* **279:** 327–329.
38. Bonen, A., J. J. Luiken, S. Liu, D. J. Dyck, B. Kiens, S. Kristiansen, L. P. Turcotte, G. J. Van Der Vusse, and J. F. Glatz. 1998. Palmitate transport and fatty acid transporters in red and white muscles. *Am. J. Physiol.* **275:** E471–E478.
39. Stremmel, W. 1988. Uptake of fatty acids by jejunal mucosal cells is mediated by a fatty acid binding membrane protein. *J. Clin. Invest.* **82:** 2001–2010.
40. Prieto, R. M., W. Stremmel, C. Sales, and J. A. Tur. 1996. Oleic acid uptake by jejunal and ileal rat brush border membrane vesicles. *Eur. J. Med. Res.* **1:** 199–203.
41. Zhou, S. L., D. Stump, D. Sorrentino, B. J. Potter, and P. D. Berk. 1992. Adipocyte differentiation of 3T3-L1 cells involves augmented expression of a 43 kDa plasma membrane fatty acid binding protein. *J. Biol. Chem.* **267:** 14456–14461.
42. Trimble, M. E. 1989. Mediated transport of long chain fatty acids by rat renal basolateral membranes. *Am. J. Physiol.* **257:** F539–F546.
43. Maniscalco, W. M., W. Stremmel, and M. Heeny-Campbell. 1990. Uptake of palmitic acid by rat alveolar type II cells. *Am. J. Physiol.* **259:** L206–L212.
44. Campbell, F. M., A. M. Clohessy, M. J. Gordon, K. R. Page, and A. K. Dutta-Roy. 1997. Uptake of long chain fatty acids by human placental choriocarcinoma (BeWo) cells: role of plasma membrane fatty acid-binding protein. *J. Lipid Res.* **38:** 2558–2568.
45. Stump, D. D., R. M. Nunes, D. Sorrentino, L. M. Isola, and P. D. Berk. 1992. Characteristics of oleate binding to liver plasma membranes and its uptake by isolated hepatocytes. *J. Hepatol.* **16:** 304–315.
46. Spector, A. A., J. E. Fletcher, and J. D. Ashbrook. 1971. Analysis of long-chain free fatty acid binding to bovine serum albumin by determination of stepwise equilibrium constants. *Biochemistry.* **10:** 3229–3232.
47. Richieri, G. V., A. Anel, and A. M. Kleinfeld. 1993. Interactions of long-chain fatty acids and albumin: determination of free fatty acid levels using the fluorescent probe ADIFAB. *Biochemistry.* **32:** 7574–7580.
48. Kono, T., F. W. Robinson, and J. A. Sarver. 1975. Insulin-sensitive phosphodiesterase. *J. Biol. Chem.* **250:** 7826–7835.
49. Stremmel, W., B. J. Potter, and P. D. Berk. 1983. Studies of albumin binding to rat liver plasma membranes: implications for the albumin receptor hypothesis. *Biochim. Biophys. Acta.* **756:** 20–27.
50. Stremmel, W., S. Kochwa, and P. D. Berk. 1983. Studies of oleate binding to rat liver plasma membranes. *Biochem. Biophys. Res. Commun.* **112:** 88–95.
51. Berk, P. D., S-L. Zhou, C-L. Kiang, D. D. Stump, and M. W. Bradbury. 1999. Selective up-regulation of fatty acid uptake by adipocytes characterizes both genetic and diet-induced obesity in rodents. *J. Biol. Chem.* **274:** 28626–28631.
52. Sorrentino, D., R. B. Robinson, C-L. Kiang, and P. D. Berk. 1989. At physiologic albumin/oleate concentrations oleate uptake by isolated hepatocytes, cardiac myocytes, and adipocytes is a saturable function of the unbound oleate concentration. *J. Clin. Invest.* **84:** 1325–1333.
53. Weisiger, R. A. 1993. The role of albumin binding in hepatic organic anion transport. *In* Hepatic Transport and Bile Secretion. N. Tavoloni and P. D. Berk, editors. Raven Press, New York. 171–196.
54. Sorrentino, D., S-L. Zhou, E. Kokkotou, and P. D. Berk. 1992. Sex differences in hepatic fatty acid uptake reflect a greater affinity of the transport system in females. *Am. J. Physiol.* **263:** G380–G385.
55. Rose, H., M. Conventz, Y. Fischer, E. Jüngling, T. Hennecke, and H. Kammermeier. 1994. Long-chain fatty acid-binding to albumin: re-evaluation with directly measured concentrations. *Biochim. Biophys. Acta.* **1215:** 321–326.
56. Bojesen, I. N., and E. Bojesen. 1994. Binding of arachidonate and oleate to bovine serum albumin. *J. Lipid Res.* **35:** 770–778.
57. Berman, M. M., and M. F. Weiss. 1967. Users' Manual for SAAM. U.S. Public Health Services Publication 1703. U.S. Department of Health and Human Services, U.S. Government Printing Office, Washington, DC.
58. Berman, M. M., E. Shahn, and M. F. Weiss. 1962. The routine fitting of kinetic data to models: a mathematical formalism for digital computer. *Biophys. J.* **2:** 275–287.
59. Kleinfeld, A. M., S. Storms, and M. Watts. 1998. Transport of long-chain native fatty acids across human erythrocyte ghost membranes. *Biochemistry.* **37:** 8011–8019.
60. Luiken, J. J. F., F. A. van Nieuwenhoven, G. J. van der Vusse, and J. F. C. Glatz. 1997. Uptake and metabolism of palmitate by isolated cardiac myocytes from adult rats: involvement of sarcolemmal proteins. *J. Lipid Res.* **38:** 745–758.
61. Trimble, M. E. 1993. Palmitate transport by rat renal basolateral membrane vesicles in the presence of albumin. *J. Am. Soc. Nephrol.* **3:** 1920–1929.
62. Cseh, R., and R. Benz. 1999. Interaction of phloretin with lipid monolayers: relationship between structural changes and dipole potential change. *Biophys. J.* **77:** 1477–1488.
63. Andersen, O. S., A. Finkelstein, I. Katz, and A. Cass. 1976. Effect of phloretin on the permeability of thin lipid membranes. *J. Gen. Physiol.* **67:** 749–771.
64. Cseh, R., M. Hetzer, K. Wolf, J. Kraus, G. Bringmann, and R. Benz. 2000. Interaction of phloretin with membranes: on the mode of action of phloretin at the water-lipid interface. *Eur. Biophys. J.* **29:** 172–183.
65. Forman, S. A., A. S. Verkman, J. A. Dix, and A. K. Solomon. 1982. Interaction of phloretin with the anion transport protein of the red blood cell membrane. *Biochim. Biophys. Acta.* **689:** 531–538.
66. Antonenko, Y. N., and A. A. Bulychev. 1991. Effect of phloretin on the carrier-mediated electrically silent ion fluxes through the bilayer lipid membrane: measurements of pH shifts near the membrane by pH microelectrode. *Biochim. Biophys. Acta.* **1070:** 474–480.
67. Kleinfeld, A. M., P. Chu, and J. Storch. 1997. Flip-flop is slow and rate-limiting for the movement of long chain anthroloxy fatty acids across lipid vesicles. *Biochemistry.* **36:** 5702–5711.
68. Gutknecht, J. 1988. Proton conductance caused by long chain fatty acids in phospholipid bilayer membranes. *J. Membr. Biol.* **106:** 83–93.
69. Schmider, W., A. Fahr, H. E. Blum, and G. Kurz. 2000. Transport of heptafluorostearate across model membranes: membrane transport of long-chain fatty acid anions. *J. Lipid Res.* **41:** 775–787.
70. Stoll, G. H., R. Voges, W. Gerok, and G. Kurz. 1991. Synthesis of a metabolically stable modified long chain fatty acid salt and its photolabile derivative. *J. Lipid Res.* **32:** 843–857.
71. Schmider, W., A. Fahr, R. Voges, W. Gerols, and G. Kurz. 1996. Irreversible inhibition of hepatic fatty acid salt uptake by photoaffinity labeling with 11,11-azistearate. *J. Lipid Res.* **37:** 739–753.
72. Skulachev, V. P. 1991. Fatty acid circuit as a physiological mechanism of uncoupling of oxidative phosphorylation. *FEBS Lett.* **294:** 158–162.
73. Garlid, K. D., D. E. Orosz, M. Mondriansky, S. Vassanelli, and P. Jesek. 1996. On the mechanism of fatty acid-induced proton transport by mitochondrial uncoupling protein. *J. Biol. Chem.* **271:** 2615–2620.

Downloaded from www.jlr.org by guest, on June 14, 2012

74. Jezek, P., J. Hanus, C. Semrad, and K. D. Garlid. 1996. Photoactivated azido fatty acid irreversibly inhibits anion and proton transport through mitochondrial uncoupling protein. *J. Biol. Chem.* **271:** 6199–6205.
75. Frohnert, B. J., and D. A. Bernlohr. 2000. Regulation of fatty acid transporters in mammalian cells. *Prog. Lipid Res.* **39:** 83–107.
76. Berk, P. D., S-L. Zhou, C-L. Kiang, D. Stump, M. Bradbury, and L. M. Isola. 1997. Uptake of long chain free fatty acids is selectively upregulated in adipocytes of Zucker rats with genetic obesity and non-insulin dependent diabetes mellitus. *J. Biol. Chem.* **272:** 8830–8835.
77. McArthur, M. J., B. P. Atshaves, A. Frolov, W. D. Foxworth, A. B. Kier, and F. Schroeder. 1999. Cellular uptake and intracellular trafficking of long chain fatty acids. *J. Lipid Res.* **40:** 1371–1383.
78. Bonen, A., J. J. F. P. Luiken, Y. Arumugam, J. F. C. Glaatz, and N. N. Tandon. 2000. Acute regulation of fatty acid uptake involves the cellular redistribution of fatty acid translocase. *J. Biochem.* **275:** 14501–14508.
79. Zhou, S-L., R. E. Gordon, M. Bradbury, D. Stump, C. L. Kiang, and P. D. Berk. 1998. Ethanol upregulates fatty acid uptake and plasma membrane expression and export of mitochondrial aspartate aminotransferase in HepG2 cells. *Hepatology.* **27:** 1064–1074.
80. Turcotte, L. P., J. R. Swenberger, M. Z. Tucker, and A. J. Yee. 1999. Training-induced elevation in $FABP_{pm}$ is associated with increased palmitate use in contracting muscles. *J. Appl. Physiol.* **87:** 285–293.
81. Tanaka, T., K. Sohmiya, and K. Kawamura. 1997. Is CD36 deficiency an etiology of hereditary hypertrophic cardiomyopathy? *J. Mol. Cell. Cardiol.* **29:** 121–127.
82. Odaib, A. A., B. L. Shneider, M. J. Bennett, B. L. Pober, M. Reyes-Mujica, A. L. Friedman, F. L. Suchy, and P. Rinaldo. 1998. A defect in the transport of long chain free fatty acids associated with acute liver failure. *N. Engl. J. Med.* **339:** 1752–1757.

Downloaded from www.jlr.org by guest, on June 14, 2012